

SOME FEATURES OF WIND WAVES IN LAKE MICHIGAN

Paul C. Liu

Great Lakes Research Center, U.S. Lake Survey, Army Corps of Engineers,
Detroit, Michigan 48226

ABSTRACT

Sets of simultaneous data of wind profiles and surface waves recorded in Lake Michigan during fall 1965 facilitated a detailed study of generation and decay aspects of wind waves. A logarithmic wind profile, fitted to data measured simultaneously at 3 or 4 anemometer heights, appears to be satisfactory. From the parameters of frictional wind velocity and roughness element computed from the logarithmic wind profile, the spectral growth of waves according to recently developed theoretical models of wave generation was predicted. The energy spectra of measured waves indicate that wave energy growth rate is, as predicted, exponential with respect to time but is 8 times larger than the predicted rate. The decay of wave spectra at a single location was qualitatively examined. The peak frequency either increased or remained constant for decreasing spectral energy. The similarity in behavior of wave spectra was demonstrated through normalization which resulted in an empirical equation for wave spectra. The measured equilibrium range in the high-frequency region of the spectra follows the f^{-5} rule.

INTRODUCTION

Along with the development of various theoretical models for the physical processes of wind-generated water waves, a number of laboratory and field measurements have been made recently. The published results of these studies show little quantitative agreement as yet between theory and experiment on wind waves. This may be because a mathematically tractable model requires drastic assumptions and simplifications, whereas the actual processes involve many physical unknowns.

In connection with the study of waves in the Great Lakes, spectral analysis of wave records from Lake Michigan, where wind profile data are simultaneously available, were obtained. The available data were recorded during a nonsteady wind field, where both speed and direction were changing with time; nonsteadiness of wind is frequent in the Great Lakes and inhibits substantial efforts to link field data with existing theoretical results. This paper presents some qualitative features of wind waves resulting from a study of Lake Michigan wave spectra. The results provide a basis for estimates of spectral growth in wave spectra over the major frequency range; this is discussed in the light of theoretical models.

DATA AND ANALYSIS

Wind and wave data

The wind profile data used in this study were reported by Elder and Soo (1967). The data were recorded in 1965 from U.S. Lake Survey's Lake Michigan Research Tower, a steel mast of braced construction extending 16 m above the water surface and located in 15 m of water about 1.6 km from the east shore of the lake near Muskegon, Michigan (Fig. 1). Anemometers were placed on the mast 4, 8, 12, and 14 m above mean water level. The published data (hourly averages) were reanalyzed in this study and fitted to logarithmic profiles. In particular, 33 sets of profiles during the period of 29 October to 1 November 1965 were used because wave records during this period were also available.

The waves were measured with a step-resistance wave gauge consisting of a 4.5-m wave staff fabricated in plastic sections with resistors spaced at 6-cm intervals. Wave data were recorded continuously (1.27 cm/min) on magnetic tape. Episodes of wave records 8 to 10 min long, selected to accord with wind data, were reproduced in analog form on strip charts through a flux responsive system reproducer at the U.S. Army Coastal Engineering Research Center, Washington, D.C. The strip-chart

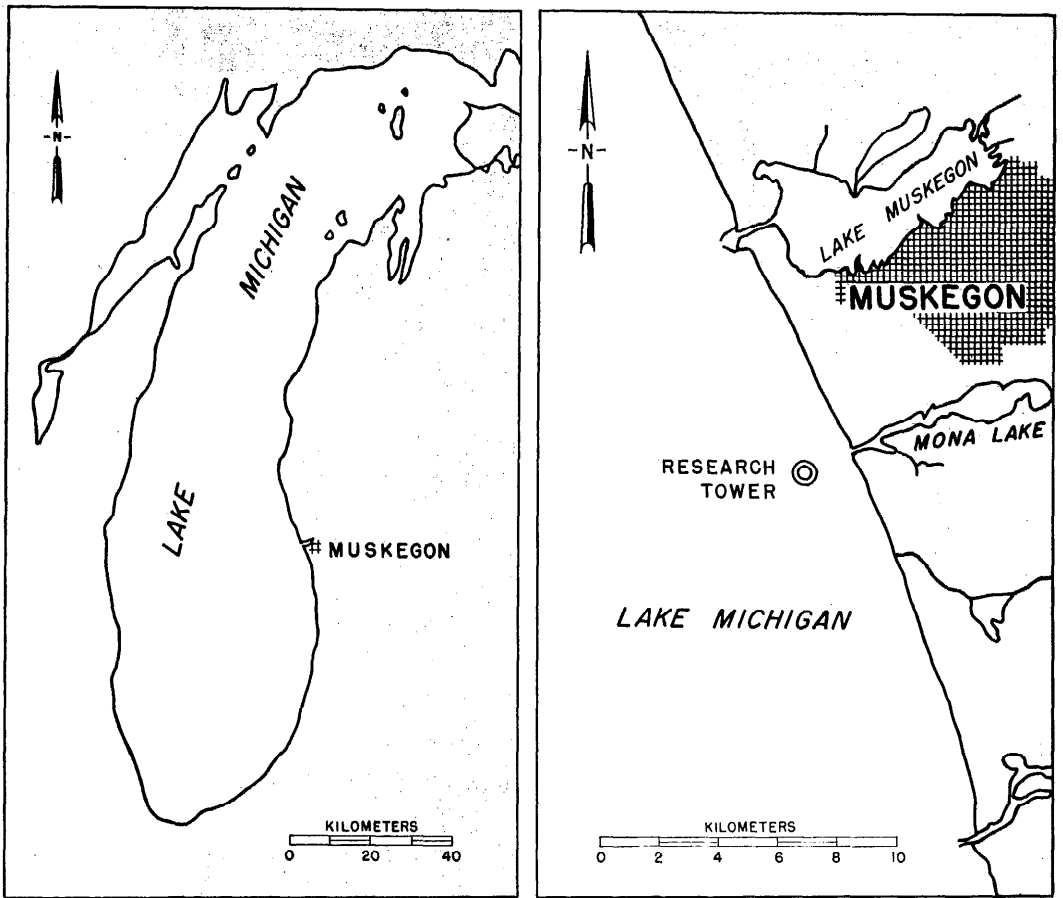


FIG. 1. Location of Lake Michigan research tower.

records were then digitized at a sampling rate of 3/sec.

Logarithmic wind profiles

The form of the wind profile has been studied extensively. The logarithmic profile is generally accepted as valid for turbulent air motion over water. Based on dimensional analysis, the vertical distribution of windspeed U with respect to height z over water is given as

$$U(z) = U_1 \ln(z/z_0), \quad (1)$$

where z_0 is the parameter of roughness, and U_1 is the reference velocity defined by

$$U_1 = U_*/\kappa = \kappa^{-1}(\tau_0/\rho_a)^{1/2}. \quad (2)$$

U_* denotes the friction velocity, κ is the nondimensional Kármán's constant assumed equal to 0.40, ρ_a is the density of air, and τ_0 is the shear stress at the water surface.

Equation (1) was fitted to the profile data using the method of least squares. The parameters U_1 and z_0 were solved simultaneously during the regression process. The resulting dimensionless profiles of windspeeds, where $U_1 = 2.5U_*$, are plotted in Fig. 2. The measured data and the line denoting the logarithmic law show fair agreement, with some indication that the value of Kármán's constant for the Great Lakes may be somewhat smaller than assumed. Earlier measurements on the Great Lakes (Portman 1960; Bruce, Anderson, and Rodgers 1961), also plotted in Fig. 2,

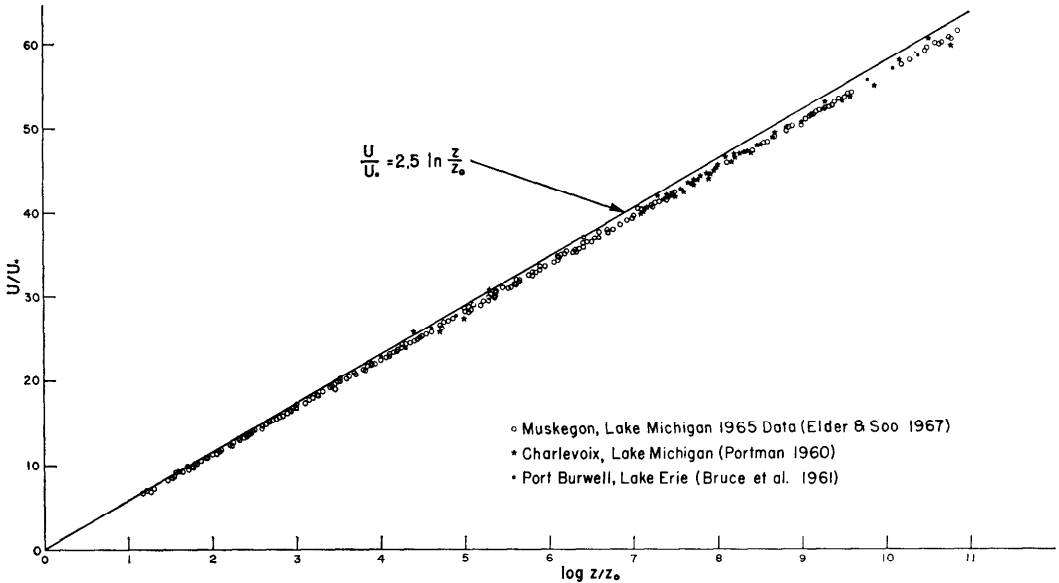


FIG. 2. Dimensionless profile of windspeed over water waves.

indicate the same result. In the absence of more accurate measurements, a logarithmic profile apparently is adequate to describe the distribution of windspeed over waves in the Great Lakes.

The data in Fig. 2 were obtained from the reported profile data without considering the effects of atmospheric stability. An examination of these effects indicates that all data lie within 1% of the linear regression line for a neutral atmosphere. For stable or unstable atmospheres, on the other hand, a maximum deviation of 3% was detected. Most of the wind profiles used in the study of waves were recorded under neutral or near-neutral conditions (i.e., temperature differences between air and water within $\pm 3C$).

Windspeeds and drag coefficients

It is customary to express the shear stress exerted by the wind on the water surface in terms of the average windspeed measured at a certain height, usually 10 m, as

$$\tau_0 = \rho_a C_{10} U_{10}^2. \quad (3)$$

The factor of proportionality C_{10} , a dimensionless constant, is known as the drag

coefficient. Because $U_*^2 = \tau_0/\rho_a$, C_{10} can be easily related to the parameters of the wind profile by

$$C_{10} = (U_*/U_{10})^2. \quad (4)$$

Using equation (1) with $z = 10$ m and equation (4), we can compute a pair of values of U_{10} and C_{10} for each profile. The problem of determining the surface stress is thus reduced to ascertaining reliable values of C_{10} .

When only wind data of neutral stability conditions are used and cases of decreasing wind are eliminated, relatively less scatter is found and unambiguous connection between C_{10} and U_{10} is obtained (Fig. 3). The solid line in the figure is a linear regression curve which can be represented by

$$C_{10} = (0.35 + 0.15U_{10}) \times 10^{-3}, \quad (5)$$

where U_{10} is in m/sec.

Although quantitatively less, the trend of data in Fig. 3, which indicates that C_{10} increases with increasing windspeed, agrees qualitatively with most recent investigations (e.g., Deacon and Webb 1962; Paulson 1967). In particular, the order of

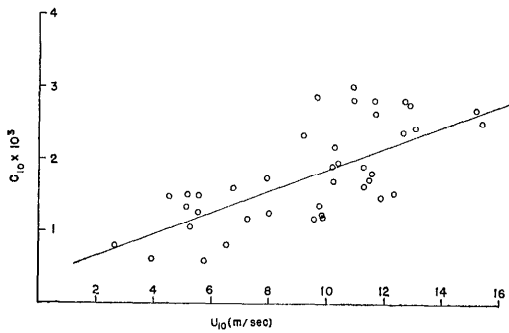


FIG. 3. The variation of drag coefficient with windspeed for neutral and near-neutral atmosphere.

magnitude of the empirical coefficients in equation (5) agrees quite closely with the results of Sheppard (1958) and Zubkovskii and Kravchenko (1967); the latter was obtained from direct measurements of momentum fluxes with an acoustic anemometer.

Spectral analysis

Spectral analysis is a convenient mathematical tool for the study of water waves. The spectra in this study were computed by the correlation-cosine transformation procedure (Blackman and Tukey 1958).

Assuming that the digitized wave records can be regarded as stationary Gaussian random processes, the autocorrelation function is given by

$$R(t_0) = \langle h(t)h(t+t_0) \rangle, \quad (6)$$

where $h(t)$ represents the time history of the water surface, and $\langle \cdot \rangle$ denotes the average with respect to time. $R(t_0)$, a function of time lag t_0 , is the temporal average of the correlation of all values of $h(t)$ that are separated in time by t_0 . For zero lag, it becomes

$$R(0) = \langle h^2(t) \rangle = \sigma^2, \quad (7)$$

where σ^2 designates the variance of the surface displacements. Physically, the variance is proportional to the average energy contained in the train of waves. The significant wave height $H_{1/3}$, defined as the average of the highest third of the wave

heights in the record, is related to the variance by $H_{1/3} = 4\sigma$ (Cole 1967).

The energy spectra were calculated by the following relation:

$$E(f) = \int_0^\infty R(t) \cos 2\pi ft \, dt. \quad (8)$$

The raw spectra thus obtained were smoothed and the noise removed by the techniques described by Liu (1968). A total of 1,600 data points was used from each set of data for the calculations. A maximum of 80 lags was used in calculating correlation functions. The 90% confidence limits were approximately 0.72 and 1.31, with respect to the spectral values.

RESULTS AND DISCUSSION

Representation of the spectral field

Following the presentations of Barnett and Wilkerson (1967) and Munk et al. (1963), a spectral field for waves was derived by plotting the contours of equal spectral density on the frequency-time axes (Fig. 4). The corresponding wind histories are also plotted to provide an overview of the variability of spectral energy of waves with respect to wind field.

The contour diagram represents the 3-day period from 0700 on 29 October through 0300 on 1 November 1965. The contours cover mainly the lower-frequency part of the spectrum, where most of the dominant energies are concentrated. The plotting interval along the frequency axis was 0.025 Hz, which gives approximately 16 values of $E(f)$ from each of the 33 spectra. Along the time axis, the plotting interval varies from 1 to 5 hr depending on the availability of wind records. Wind data are plotted and represented by solid lines, with the exception of two large gaps of 1400–2200 hours on 29 October and 0800–1400 hours on 31 October which are shown by dotted lines. Continuity and linear variations were assumed between the discrete data points; this seems justified in view of the variations of corresponding spectral fields.

An examination of the spectral field versus wind field indicates that for increas-

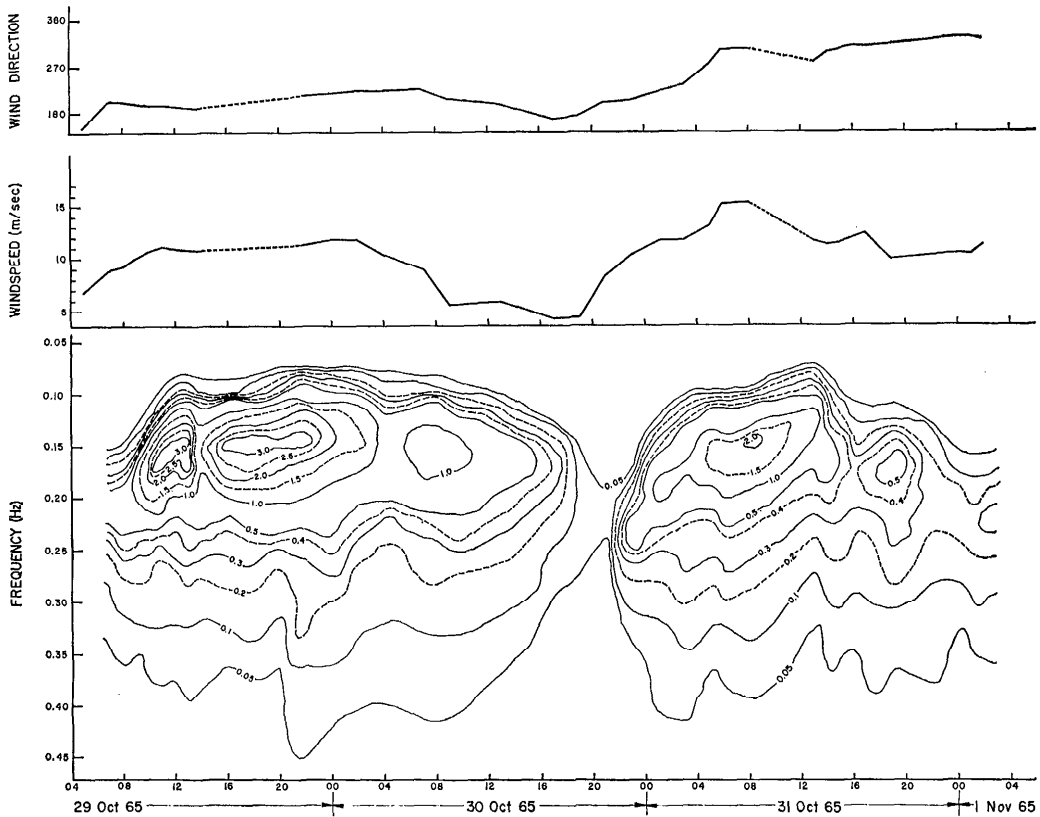


FIG. 4. Contours of equal spectral energy density ($\text{m}^2\text{-sec}$) on a frequency-time plot, and corresponding wind direction and speed.

ing windspeed, the major spectral peaks migrate toward lower frequencies. This is analogous to what is expected from a theoretical model of "switching on" a steady wind over a large body of water for an increasing duration or fetch. The variations of wind direction appear to have less qualitative effect over the spectral field than does the windspeed. However, a constantly changing wind direction causes a low intensity of spectral energy compared to a steady wind direction of lower speed. It is obvious that the actual mechanism of wave growth differs markedly between winds with varying direction and those with steady direction.

Several ridges appear in the higher frequency region of the spectral field. These ridges approximately parallel the frequency

axis and more or less correlate with energy peaks which, in turn, closely correspond to the peaks of windspeed. This illustrates that the spectral field of waves is very sensitive to the wind field and that the wave spectra are directly affected by the instantaneous wind variations.

The growth of wave spectra

Since the first analyses of Miles (1957) and Phillips (1957) on the generation of wind waves were published over a decade ago, there have been many significant contributions to further advances in modern wind-wave theory (for reviews see Kinsman 1965; Sandover and Holmes 1966; Phillips 1966).

In this study, attention is directed to the generalized model by Miles (1960) and

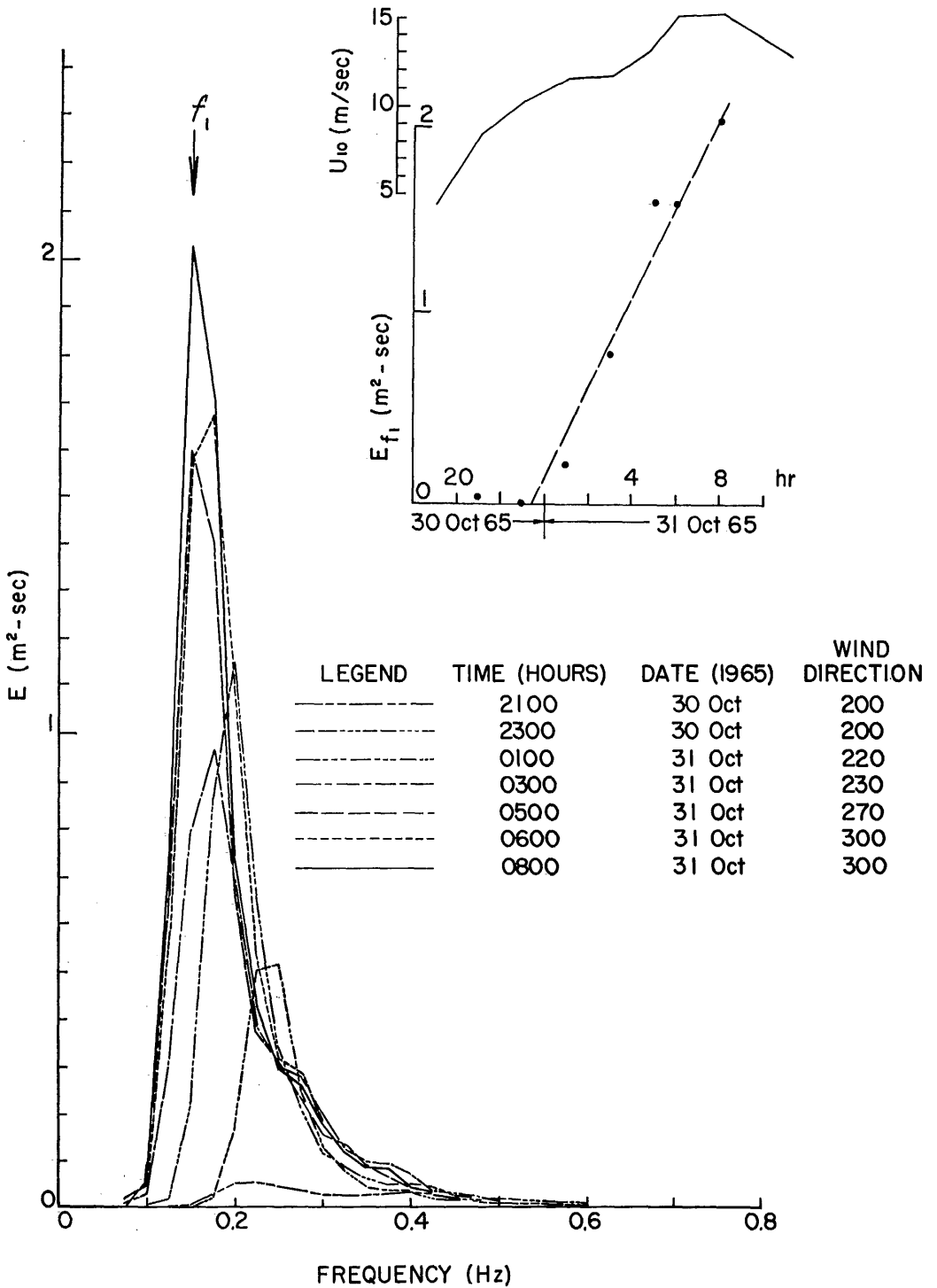


FIG. 5. The growth of wave spectrum under increasing windspeed and varying wind direction. The arrow f_1 indicates the frequency of maximum attained energy. The figure inset shows the wind history and the growth of the spectral energy component at frequency f_1 .

Phillips (1966). This model combined the resonance mechanism (Phillips 1957) of wave generation with the shear-flow model (Miles 1957) to give a quantitative theory for the growth of waves over a limited range of time. According to this model, the wave growth rate is linear in the very early stages, followed by a transition to exponential in the later stages. Laboratory studies seem to substantiate this result qualitatively (Hidy and Plate 1966; Sutherland 1968). In a previous study of Lake Michigan waves (Liu 1968), there was some indication of exponential rate in spectral growth. The data of this study were used to continue investigations of the applicability of this model.

According to Phillips (1966), the instantaneous wave-number spectrum for wave energy measured at a fixed point can be expressed by

$$\psi(\mathbf{k}, t) = [\pi \Pi(\mathbf{k}, f) / (\rho_w c)^2] \times \sinh 2\pi f \zeta t / 2\pi f \zeta, \quad (9)$$

where ρ_w is the water density, c is the phase speed of waves, and \mathbf{k} is the wave number vector where $\psi(\mathbf{k}) = \psi(k, \theta)$ with θ being the direction of wave propagation and k the one-dimensional wave number associated with wave frequency by $2\pi f = (gk)^{1/2}$. The term $\Pi(\mathbf{k}, f)$ represents the wave-number-frequency spectrum of the atmospheric pressure fluctuations with respect to t . The dimensionless constant ζ , interpreted as the fractional increase in mean energy per radian-cycle, can be evaluated if the wind profile is known (Miles 1960).

To facilitate the application of the results obtained from this study, the one-dimensional frequency spectrum $E(f, t)$ rather than directional wave-number spectrum $\psi(\mathbf{k}, t)$ is used (Hidy and Plate 1966; Sutherland 1968). For waves with small amplitude the frequency spectrum function is given by

$$E(f, t) = [2(2\pi f)^3 / g^2] \psi(\mathbf{k}, t). \quad (10)$$

Let

$$F(\mathbf{k}, f) = [(2\pi)^4 f^3 / (\rho_w g c)^2] \Pi(\mathbf{k}, f), \quad (11)$$

then equation (10) becomes

$$E(f, t) = F(\mathbf{k}, f) \sinh 2\pi f \zeta t / 2\pi f \zeta. \quad (12)$$

Assuming that the spectrum of atmospheric pressure is independent of time, then $F(\mathbf{k}, f)$ is also independent of time. The differentiation of the logarithm of equation (12) with respect to time then yields the theoretical rate of energy change S_T

$$S_T = \partial \ln E / \partial t = 2\pi f \zeta \coth 2\pi f \zeta t. \quad (13)$$

Equation (13) can be used to estimate the growth rate of measured spectral components. For the cases when $2\pi f \zeta t$ is sufficiently large, equation (13) reduces to

$$\partial \ln E / \partial t = 2\pi f \zeta \quad \text{for} \quad 2\pi f \zeta t \gg 1. \quad (14)$$

When $2\pi f \zeta t$ is sufficiently small, equation (12) becomes

$$E(f, t) = F(\mathbf{k}, f) t \quad \text{for} \quad 2\pi f \zeta t \ll 1. \quad (15)$$

Since $F(\mathbf{k}, f)$ is independent of time, equation (15) indicates that theoretically $E(f, t)$ increases linearly with time.

As can be seen from Fig. 4, there are only two episodes of wave data that display the nature of growing. Figure 5 shows the plot of individual wave-frequency spectra obtained from 2100 on 30 October through 0800 on 31 October. The wind field concerned is quite unsteady. Wind direction changed constantly while wind speed increased from 5 to 15 m/sec over the 12-hr period. The changing wind direction resulted in constantly decreasing fetches involving a wave-generating mechanism yet to be understood. During that period the spectral peak generally moves toward lower frequencies. However, the growth of peak energy does not reveal a clear pattern. In the figure inset, the spectral components of energy at the frequency f_1 are plotted versus time, where f_1 is the frequency at which maximum energy is attained during this episode. A dashed line plotted through the scattered points suggests an approximate linear growth rate for this energy component. Since the linear growth implies the early stage of wave growth under a steady wind, the growth

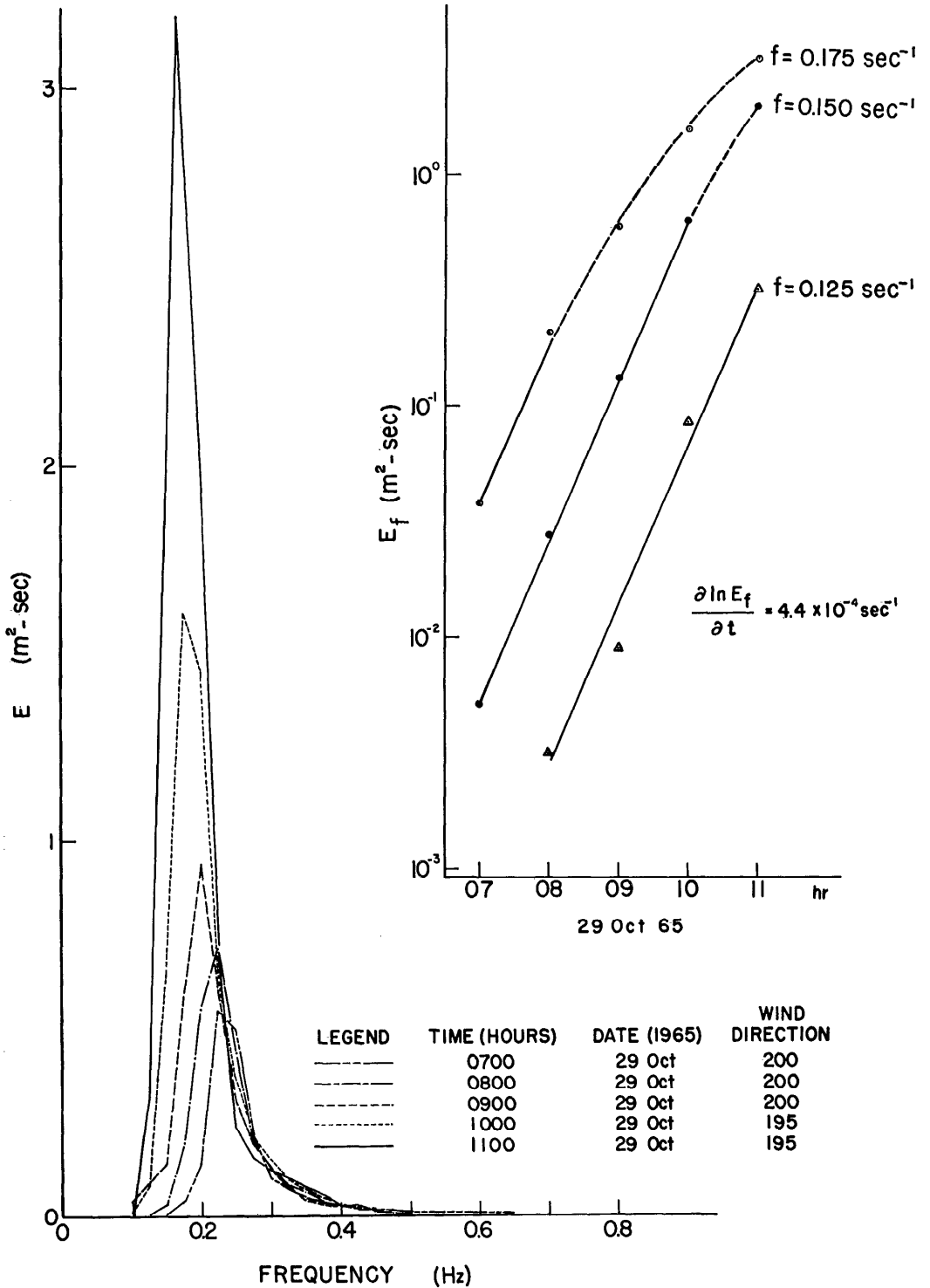


FIG. 6. The growth of wave spectrum under increasing windspeed and constant fetch. The figure inset shows the exponential growth of spectral energy components at selected low frequencies.

of wave spectra under direction-changing wind may be analogous to some kind of resonance between the waves and the exciting turbulent pressure fluctuations.

The other episode of growing waves, covering a shorter period (0700 through 1100 hours on 29 October), presents a much better basis for study in the light of theoretical analysis. The wind direction was essentially constant, and the wind-speed increased linearly from 8.9 to 11.2 m/sec over the 5-hr period. The wave spectra obtained under this wind field are plotted in Fig. 6. The results illustrate a recognizable pattern of wave growth. The spectra are sharp crested, and their shapes remain similar. The peak energy continually increases, and the front face of the spectra moves progressively toward lower frequencies as time goes on. At the high frequency side of the spectra, a region of saturated state exists where all corresponding spectral values are clustered together independent of time or windspeed. This region, representing an equilibrium between energy input and energy loss during the generating process, is known as the equilibrium range of the wave spectrum. Qualitatively, this observed behavior closely resembles the features expected from the theoretical model assuming constant windspeeds.

In the inset of Fig. 6, spectral components of energy at three low frequencies are plotted against time on a semilogarithmic scale. Although the dashed lines indicate some curved trend at a later time, the solid lines clearly demonstrate the evidence of exponential growth of the spectral energy components. The slope of these lines provides the observed logarithmic growth rate of $4.4 \times 10^{-4} \text{ sec}^{-1}$; this value will be used in comparison with theoretical calculations in the next section. The curved trend may indicate the "overshoot" behavior of the spectral energy components (Barnett and Sutherland 1968). However, the wind decayed too soon to give further evidence for this phenomenon.

From the discussions of equations (14) and (15), it is evident that the parameter

ζ is of central importance in defining the time history of each spectral energy component. The determination of ζ involves intricate analysis of the interactions between wind and waves. Several alternative mechanisms are presented in the literature, each being applicable under specified conditions. In this study, the inviscid shear-flow model of Miles (1957) is used, which requires only the wind profile and the wave spectrum to carry out the theoretical calculations.

The central concept of Miles' model is the existence of a "critical layer"—the elevation above the water surface at which the mean windspeed equals the phase speed of the wave perturbation. When the logarithmic wind profile of equation (1) is used and setting $U = c$, the height of the critical layer z_0 is

$$z_0 = z_0 \exp(c/U_1). \quad (16)$$

At this height, the energy is extracted from the wind and transferred downward to the waves. The rate of energy input to the waves is proportional to the curvature of wind profile at this critical layer. Miles (1957) has introduced a dimensionless parameter β and obtained the following relation for logarithmic wind profile

$$\zeta = (\rho_a/\rho_w)(U_1/c)^2\beta, \quad (17)$$

where β is a function of kz_0 and k denotes the wave number. The value of β for the corresponding value of kz_0 can be obtained from the curve provided by Miles (1959), and ζ is readily computed from equation (17). The data of 29 October and appropriate parameters computed for the spectra of Fig. 6 are given in Table 1, the last column of which represents the theoretically predicted growth rate of spectral energy components computed by equation (14). The phase speeds c are associated with the peak energy of each spectrum. The elapsed times t after the onset of the wind are not as clearly defined as are the fetches in this case. For a wave component in a linearized model, Phillips (1958) has demonstrated theoretically that t is dynamically equivalent to a fetch distance D

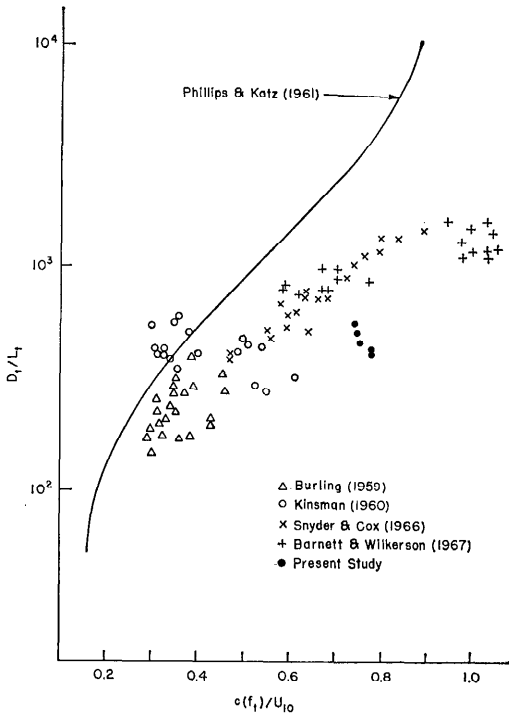


FIG. 7. Transition fetch distance, expressed in wave lengths, of the waves undergoing transition as a function of c/U . Data points of various investigators are from Barnett and Wilkerson (1967).

by $D = ct/2$, where $c/2$ —the deep-water group velocity—is the speed of energy propagation of the spectral energy components. From this, the t values in Table 1 were estimated. A comparison of the slope given in Fig. 6 with the theoretical slope, listed as S_T in Table 1, indicates that the observed growth rate is greater than that theoretically predicted rate by a factor of 8.

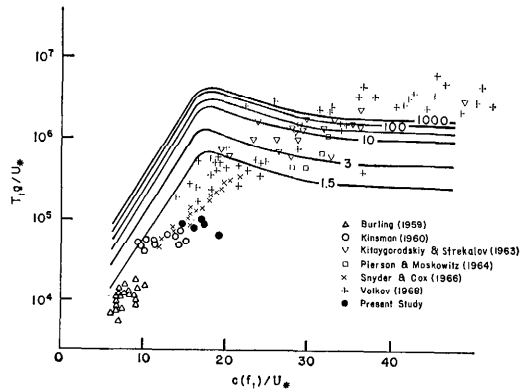


FIG. 8. The amplification factor $\sinh 2\pi f \zeta t / 2\pi f \zeta t$ as functions of normalized transition time and speed ratio. Curves are from Phillips (1966); data points of various investigators are from Volkov (1968).

This underestimation of Miles' inviscid shear-flow model in calculating spectral energy growth rate is by no means unexpected. Laboratory and field experiments reported previously have all indicated similar conclusions. The main difficulty lies perhaps in the fact that the idealized model is unable to tackle the inseparable effects within the wave field, such as wave breaking, dissipation, and nonlinear interactions between waves. The factor of 8 obtained in this study is consistent in order of magnitude with the results of Snyder and Cox (1966) and Barnett and Wilkerson (1967). This study, however, represents the only analysis of field measurements that uses measured logarithmic wind profiles.

As seen from equation (12), the expression $2\pi f \zeta t$ represents an important factor in the wave-growth mechanism. In the

TABLE 1. Data of 29 October 1965 and parameters for theoretical prediction of spectral energy growth of wind waves

Hour	U_{10} (m/sec)	U_* (m/sec)	z_0 (cm)	$H_{1/3}$ (m)	c (m/sec)	z_c (m)	kz_0	β	ξ $\times 10^5$ (rad $^{-1}$)	t $\times 10^{-4}$ (sec)	S_T $\times 10^5$ (sec $^{-1}$)
0700	8.9	0.47	0.44	1.2	7.0	1.8	0.36	0.9	3.3	5.2	4.7
0800	9.4	0.42	0.10	1.5	7.0	0.8	0.16	1.7	4.9	5.2	6.8
0900	10.0	0.46	0.13	1.5	7.7	1.1	0.17	1.6	4.6	4.5	5.9
1000	10.7	0.49	0.14	1.9	8.5	1.4	0.18	1.5	3.9	3.5	4.8
1100	11.2	0.54	0.19	2.1	8.5	1.0	0.13	1.8	5.9	3.5	6.6

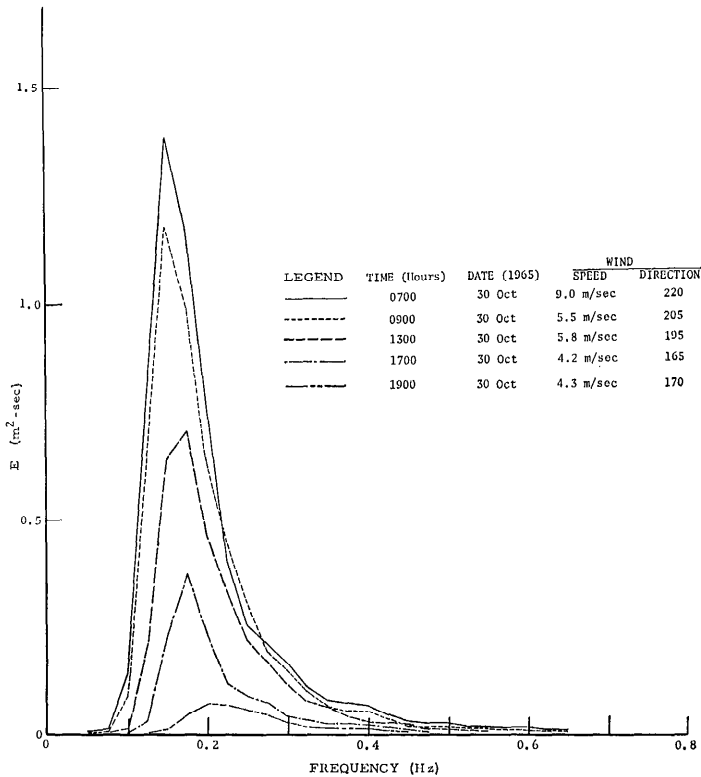


FIG. 9. The decay of wave spectrum under decreasing windspeeds.

early stages of wave growth, $2\pi f\zeta t \ll 1$, the components of the wave energy spectrum grow linearly with time. As the wind duration increases, the rate of growth for a given wave frequency changes from a linear increase to an exponential one, and $2\pi f\zeta t \gg 1$. Thus, a transition will occur for a duration t when $2\pi f\zeta t$ is of the order of unity. Based on this concept, Phillips and Katz (1961) defined a transition wind duration T_t for each frequency by

$$T_t(f) = (2\pi f\zeta)^{-1}. \quad (18)$$

To relate the transition to an observable property of wave spectra, they suggested that the time at which a particular wave component occupies the steep forward face of the energy spectrum is about equal to the transition time. Using the Miles numerical value for ζ , Phillips and Katz derived a theoretical relation and displayed the result as the transition fetch distance

in wave length (D_t/L_t) versus the speed ratio of wave phase speed and windspeed $[c(f_t)/U_{10}]$ shown in Fig. 7. The subscript t denotes that the parameters are associated with transition. The lower part of the theoretical curve in Fig. 7 generally corresponds with the measurement of Burling (1959) and Kinsman (1960) under moderate wind and short fetch. However, for measurements under stronger wind, the data of Snyder and Cox (1966) and Barnett and Wilkerson (1967) have shown a significant deviation from the theory. My data, which do not concur with the theory, are compatible in order of magnitude with those of other investigators shown in Fig. 7. As the theoretical curve was based on Miles' ζ value, which results in S_T 8 times smaller than measured, the diverging trend between theoretical and measured results is not surprising.

In a continued analysis of equation (9),

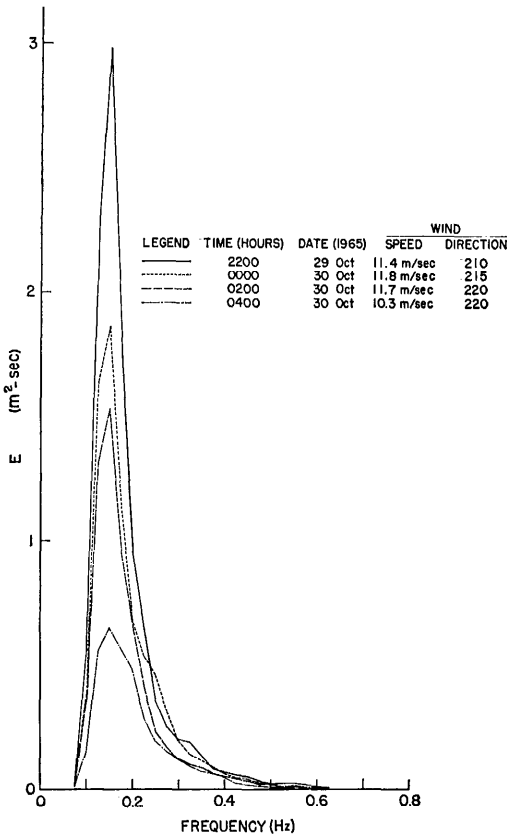


FIG. 10. The decay of wave spectrum under constant windspeed.

Phillips (1966) amended the work of Phillips and Katz (1961) by a generalized model for momentum flux. This model, considering the effect of the undulatory turbulent air flow over waves, will presumably produce additional contributions to the parameter ζ . The theoretical results on transition are shown in Fig. 8, where the amplification factors of $\sinh 2\pi f \zeta_1 t / 2\pi f \zeta_1 t$ are plotted as functions of speed ratio $c(f_t)/U_*$ versus normalized transition time $T_t g/U_*$. Here ζ_1 represents the value estimated by Phillips (1966). In an analysis of fully developed ocean waves, Volkov (1968) compared the theoretical curves in Fig. 8 with the field measurements in the western Mediterranean Sea and the data of Kitaygorodskiy and Strekalov (1962, 1963), Pierson and Moskowitz (1964), and Snyder

and Cox (1966). The results show only a qualitative agreement between theory and observation. My data are also shown in the figure, and fit closely with other field data. For all measured data with values of c/U_* in the range of 7 and 20, values of $T_t g/U_*$ are located consistently below the theoretical curves. This can be explained by the fact that for c/U_* less than 20, the value of the coupling parameter ζ_1 estimated by Phillips has practically the same value as Miles' ζ , which, as previously indicated, is too low for an oceanographic scale. A quantitative agreement between theory and observations is yet to be accomplished.

The decay of wave spectra

The behavior of a decaying wave spectrum has received relatively little attention. No relationships have been developed to show how the wave spectrum decays with respect to time at a single location. The decay studies in the literature are for waves that spread out from a generating area into a calm region (e.g., Sverdrup and Munk 1947). Under this condition, an increase in wave period is associated with the decrease of wave energy. In this study, the spectral field interpolated for the period of missing record between 0800 and 1400 hours on 31 October (Fig. 4), seems to agree qualitatively with the criterion. However, the three sets of spectra that are decaying with respect to time (shown in Figs. 9, 10, and 11) reveal that the frequency of peak energy either remains constant or increases with the decreasing wave energy. This is just opposite to the general criterion of wave decay. Although there seems no valid interpretation for this consequence, a previous study by Ijima (1957) gave similar results.

Although the spectra in Fig. 9 correspond to a decreasing windspeed with varying wind directions, the winds for the spectra in Figs. 10 and 11 are essentially constant. These quite different wind conditions imply varied decaying processes, and an examination of the results shows that the decay of the peak energy of the spectrum

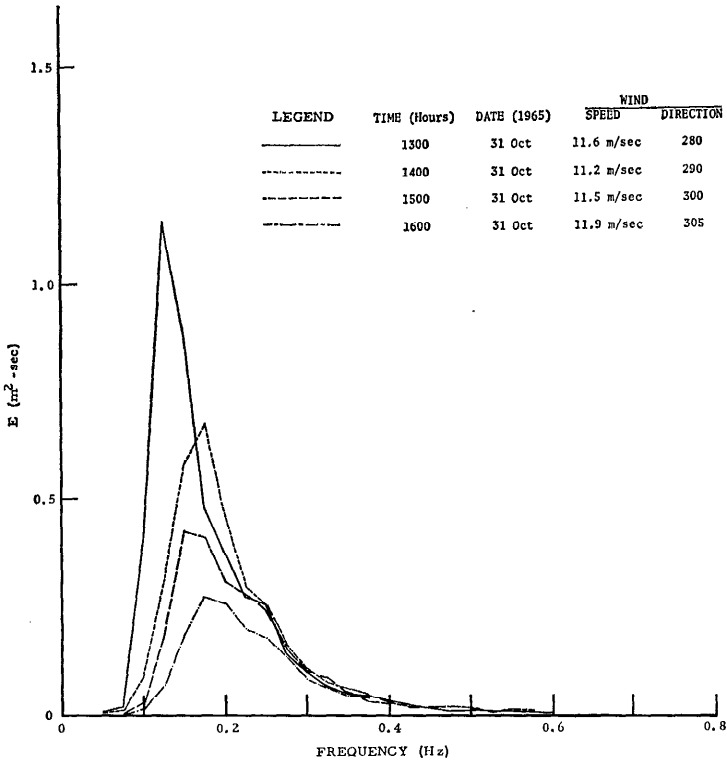


FIG. 11. The decay of wave spectrum under constant windspeed.

follows an approximate linear rate with respect to time for decreasing windspeed and an exponential rate of decay for constant windspeed.

Similarity of wave spectrum and equilibrium range

Similarity analysis is one of the elementary tools for studying measured wave spectra. The analysis establishes the dependence of the spectrum on various wave-generating factors. Using a simple normalization indicated by Hidy and Plate (1966), Liu (1968) demonstrated the similarity characteristics of wave spectra by the following expression

$$E(f)f_m/\sigma^2 = F(f/f_m), \quad (19)$$

where f_m denotes the frequency at which the spectral energy $E(f)$ is a maximum, σ^2 is the variance of the water surface, and $F(f/f_m)$ represents a dimensionless func-

tion that is universal for the spectrum of wave energy. A typical application of equation (19) to the spectra observed in this study is shown in Fig. 12. The 11 normalized spectra clearly displayed the behavior of similarity.

Defining the statistical properties of wave parameters in terms of the moments of the spectrum, Strekalov (1965) has derived a generalized spectral formula which, using the present notation, is

$$E(f) = G_1(H_0^2/f_0)(f_0/f)^a \times \exp[-G_2(f_0/f)^b], \quad (20)$$

where the subscript 0 denotes averaged parameters, and G_1 , G_2 , a , and b are dimensionless numbers empirically determinable. If linear relations exist between H_0 and σ , and f_0 and f_m , then equation (20) can be rewritten as

$$E(f) = A(\sigma^2/f_m)(f/f_m)^{-a} \times \exp[-B(f/f_m)^{-b}], \quad (21)$$

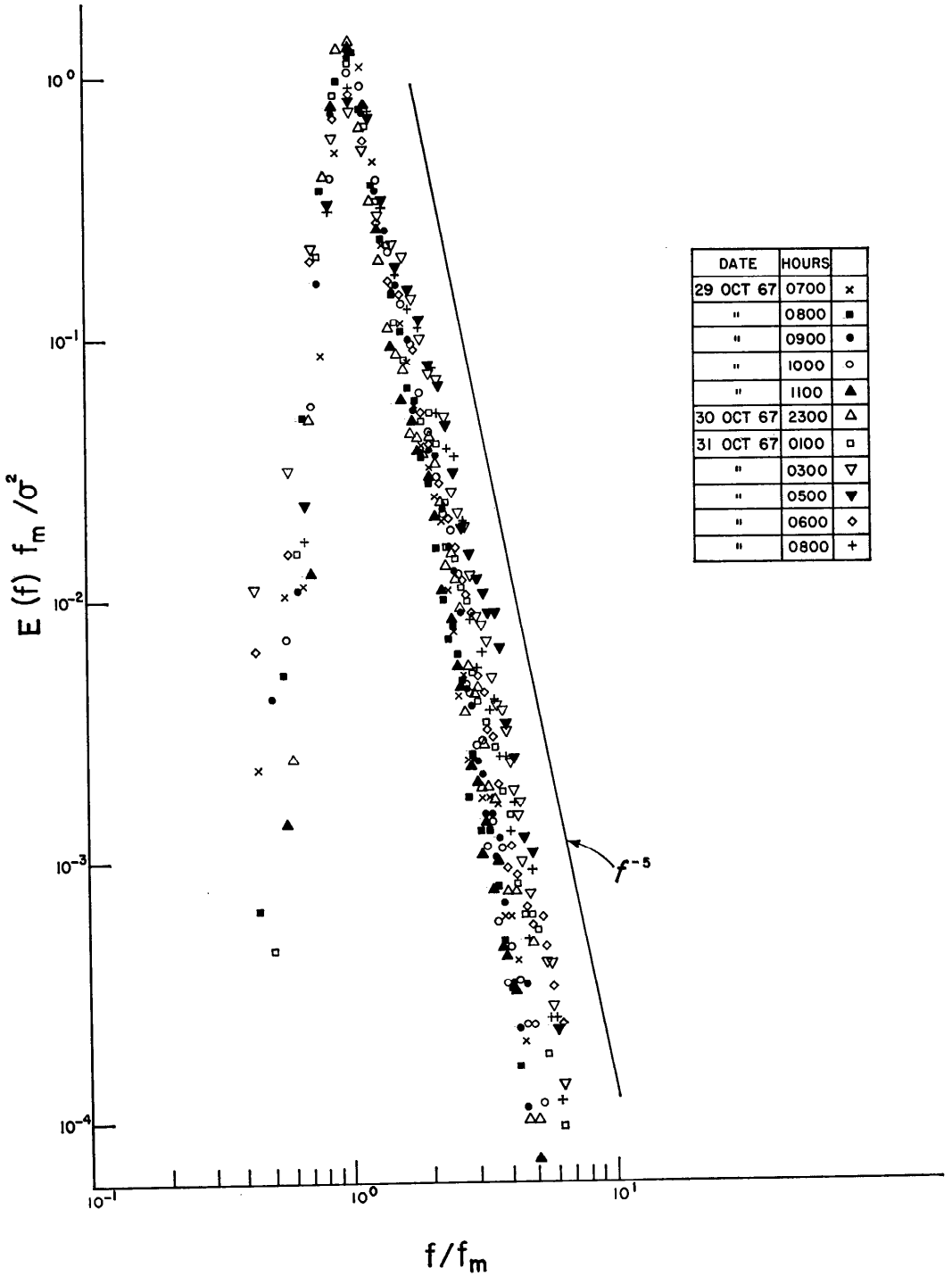


FIG. 12. The normalized wave spectra.

which is practically the quantitative form of equation (19). Fitting equation (21) to the data of Fig. 12 then leads to the following empirical equation of wave spectrum

$$E(f) = 2.6(\sigma^2/f_m)^{-5} \exp[-0.94(f/f_m)^{-4}], \quad (22)$$

which indicates that on the high frequency side of the spectrum, $E(f)$ is proportional to f^{-5} . This is the region of the "equilibrium range" representing the saturation state of waves as first introduced by Phillips (1958). The two negative exponents of (f/f_m) , namely -5 and -4 , are in agreement with the spectrum developed by Bretschneider (1959) and the one proposed by Pierson and Moskowitz (1964) for fully developed seas. The application of similarity analysis to substantiate the f^{-5} rule seems more appropriate than the process of averaging spectra generally employed.

The parameters σ and f_m can be obtained from directly observable quantities H_0 and f_0 , respectively. Therefore equation (22) can be used to estimate a wave spectrum where actual wave recordings are not available. With the empirical relations between wind and H_0 and f_0 available, equation (22) can also be used for hindcasting wave spectra directly from wind data.

REFERENCES

- BARNETT, R. P., AND A. J. SUTHERLAND. 1968. A note on an overshoot effect on wind-generated waves. *J. Geophys. Res.* **73**: 6879-6885.
- , AND J. C. WILKERSON. 1967. On the generation of ocean wind waves as inferred from airborne measurements of fetch-limited spectra. *J. Marine Res.* **25**: 292-328.
- BLACKMAN, R. B., AND J. W. TUKEY. 1958. *The measurement of power spectra*. Dover, New York. 190 p.
- BRETSCHNEIDER, C. L. 1959. Wave variability and wave spectra for wind generated gravity waves. U.S. Army Corps Eng., Beach Erosion Bd. Tech. Mem. 118. 192 p.
- BRUCE, J. P., D. V. ANDERSON, AND G. K. RODGERS. 1961. Temperature, humidity, and wind profiles over the Great Lakes. *Proc. Conf. Great Lakes Res.*, 4th, Great Lakes Res. Div., Inst. Sci. Technol., Mich. Univ., Publ. 7, p. 65-70.
- BURLING, R. W. 1959. The spectrum of waves at short fetches. *Deut. Hydrograph. Z.* **12**: 45-64, 96-117.
- COLE, A. L. 1967. Wave hindcasts vs. recorded waves. *Univ. Mich. Rep.* 06768-2-F, Suppl. 1. 88 p.
- DEACON, E. L., AND E. K. WEBB. 1962. Small-scale interactions in the sea, p. 43-87. *In* M. N. Hill [ed.], *The sea*, v. 1. Interscience.
- ELDER, F. C., AND H. K. SOO. 1967. An investigation of atmospheric turbulent transfer processes over water. *Mich. Univ., Great Lakes Res. Div. Spec. Rep.* 29. 46 p.
- HIDY, G. M., AND E. J. PLATE. 1966. Wind action on water standing in a laboratory channel. *J. Fluid Mech.* **26**: 651-587.
- IJIMA, T. 1957. The properties of ocean waves on the Pacific coast and the Japan Sea coast of Japan. *Transp. Tech. Res. Inst., Tokyo, Rep.* 25. 87 p.
- KINSMAN, B. 1960. Surface waves at short fetch and low wind speed—a field study. *Chesapeake Bay Inst., Tech. Rep.* 19. 581 p.
- . 1965. *Wind waves*. Prentice-Hall, Inc., Englewood Cliffs, N.J. 676 p.
- KITAYGORODSKIY, S. A., AND S. S. STREKALOV. 1962. Contribution to an analysis of the spectra of wind caused wave action I. *Bull. Acad. Sci. USSR, Geophys. Ser.* **1962**(9): 765-769.
- , AND ———. 1963. On the analysis of spectra of wind-generated wave motion II. *Bull. Acad. Sci. USSR, Geophys. Ser.* **1963**(3): 754-760.
- LIU, P. C. 1968. Spectral analysis of shallow water waves in Lake Michigan. *Proc. Annu. Conf. Great Lakes Res.* **1968**: 412-423.
- MILES, J. W. 1957. On the generation of surface waves by shear flows. *J. Fluid Mech.* **6**: 568-582.
- . 1959. On the generation of surface waves by shear flows. Part 2. *J. Fluid Mech.* **6**: 568-582.
- . 1960. On the generation of surface waves by turbulent shear flows. *J. Fluid Mech.* **7**: 469-478.
- MUNK, W. II., G. R. MILLER, F. E. SNODGRASS, AND H. F. BARBER. 1963. Directional recording of swell from distant storms. *Phil. Trans. Roy. Soc. London, Ser. A* **255**: 505-584.
- PAULSON, C. A. 1967. Profiles of wind speed, temperature and humidity over the sea. *Dep. Atmos. Sci., Univ. Wash., Seattle. Sci. Rep.* NSF GP-2418. 128 p.
- PHILLIPS, O. M. 1957. On the generation of waves by turbulent wind. *J. Fluid Mech.* **2**: 417-445.
- . 1958. The equilibrium range in the spectrum of wind generated waves. *J. Fluid Mech.* **4**: 426-433.
- . 1966. *The dynamics of the upper ocean*. Cambridge. 261 p.

- , AND E. J. KATZ. 1961. The low frequency components of the spectrum of wind-generated waves. *J. Marine Res.* **19**: 57-69.
- PIERSON, W. J., JR., AND L. MOSKOWITZ. 1964. A proposed spectral form for fully developed wind seas based on the similarity theory of S. A. Kitaygorodskiy. *J. Geophys. Res.* **69**: 5181-5190.
- PORTMAN, D. J. 1960. An improved technique for measuring wind and temperature profiles over water and some results obtained for light winds. *Proc. Conf. Great Lakes Res.*, 3rd, Great Lakes Res. Div., Inst. Sci. Technol., Mich. Univ., Publ. 4, p. 77-84.
- SANDOVER, J. A., AND P. HOLMES. 1966. Water waves generated by an air stream—a literature survey. *Houille Blanche* **6**: 734-743.
- SHEPPARD, P. A. 1958. Transfer across the earth's surface and through the air above. *Quart. J. Roy. Meteorol. Soc.* **84**: 205-224.
- SNYDER, R. L., AND C. S. COX. 1966. A field study of the wind generation of ocean waves. *J. Marine Res.* **24**: 141-178.
- STREKALOV, S. S. 1965. Dependence of the energy spectrum of a locally generated wave train. *Oceanology (USSR)* **5**: 17-27.
- SUTHERLAND, A. J. 1968. Growth of spectral components in a wind-generated wave train. *J. Fluid Mech.* **33**: 545-560.
- SVERDRUP, H. V., AND W. H. MUNK. 1947. *Wind, sea and swell: Theory of relations for forecasting.* U.S. Navy Hydrogr. Office Publ. 601. 44 p.
- VOLKOV, Y. A. 1968. Analysis of the spectra of sea swell developing under the action of turbulent wind. *Izv. Acad. Sci. USSR Atmos. Oceanic Phys.* **4**: 555-564.
- ZUBKOVSKII, S. L., AND T. K. KRAVCHENKO. 1967. Direct measurements of some characteristics of atmospheric turbulence in the near-water layer. *Izv. Atmos. Oceanic Phys. Acad. Sci. USSR* **3**: 127-135.